

Effect of High Ion Temperature on the Polytopic Coefficient in the End Region of GAMMA 10/PDX^{*})

Kunpei NOJIRI, Mizuki SAKAMOTO, Naomichi EZUMI, Satoshi TOGO, Takaaki IIJIMA, Seowon JANG, Akihiro TERAKADO, Yosuke KINOSHITA, Toshiki HARA, Tomonori TAKIZUKA¹⁾, Yuichi OGAWA²⁾ and Yousuke NAKASHIMA

Plasma Research Center, University of Tsukuba, Tsukuba 305-8577, Japan

¹⁾*Graduate School of Engineering, Osaka University, Suita 565-0871, Japan*

²⁾*Graduate School of Frontier Sciences, University of Tokyo, Kashiwa 277-8568, Japan*

(Received 30 September 2018 / Accepted 9 January 2019)

The effect of high ion temperature on the ion polytopic coefficient (γ) was experimentally investigated in the end region of the GAMMA 10/PDX tandem mirror. The ion temperature parallel to the magnetic field (T_{\parallel}) was varied using the ion cyclotron range of frequencies (ICRF) waves, which heat the plasma in the central cell, and by applying an additional gas puff in the central cell. Assuming the ion sound speed, γT_{\parallel} was evaluated by a Langmuir probe, and T_{\parallel} was evaluated in an ion energy analyzer. These parameters were combined to evaluate γ . The time evolutions of γT_{\parallel} obtained from the probe and T_{\parallel} obtained from the energy analyzer were similar. The plasma in the end region can be regarded as collisionless, but γ was lower with ICRF heating than without the heating. A high T_{\parallel} component was identified in the heated case. As mentioned in a previous numerical study [B. Lin *et al.*, Phys. Plasmas **23**, 083508 (2016)], it is experimentally suggested that γ can be reduced by the high T_{\parallel} component resulting from the ICRF heating.

© 2019 The Japan Society of Plasma Science and Nuclear Fusion Research

Keywords: ion temperature, ion polytopic coefficient, sound speed, Langmuir probe, ion energy analyzer

DOI: 10.1585/pfr.14.2401086

1. Introduction

The ion sound speed (C_s) [1–3] is an important parameter in boundary plasma physics related to sheath phenomena. It is a function of the electron temperature T_e , the ion temperature parallel to the magnetic field T_{\parallel} , and the ion polytopic coefficient γ . Specifically, $C_s = \{(kT_e + \gamma kT_{\parallel})/m_i\}^{1/2}$, where k is the Boltzmann constant [2,3]. Theoretical and numerical studies using plasma fluid models have shown that the sheath characteristics are affected by ion temperature T_i [4–7] and γ [8]. In a one-dimensional (1D) particle model, the authors of [9] also showed that the hot T_{\parallel} component, which is higher than T_e , imparts strong kinetic effects and reduces the γ in collisionless plasma below the widely used value in 1D adiabatic flow, where the temperature is anisotropic and $\gamma = 3$ in the flow direction. However, as experimental investigation of this phenomenon is lacking, investigating the effect of high T_{\parallel} on γ and C_s is important.

Langmuir probes (LPs) are widely used for measuring basic plasma parameters such as T_e , the electron density (n_e), and ion particle flux. The drift speed of ions flowing into the LP reaches C_s and the ion saturation current reflects the value of C_s . Therefore, when T_{\parallel} is non-

negligible compared to T_e , there is a possibility to evaluate γT_{\parallel} using the LP.

GAMMA 10/PDX is a tandem mirror device in which the plasma T_i exceeds the plasma T_e [10, 11]. In a typical discharge, T_i exceeds T_e by one order of magnitude or more. Furthermore, T_i can be varied by applying the heating system using the ion cyclotron range of frequencies (ICRF).

In this study, we attempt to evaluate the effect of high T_{\parallel} on γ using an LP and an ion energy analyzer in the end region of GAMMA 10/PDX.

2. Experimental Device and Diagnostics

2.1 GAMMA 10/PDX tandem mirror

Figure 1 shows schematics of (a) part of the GAMMA 10 tandem mirror and (b) its magnetic field. The device consists of a central cell, anchor cells, plug/barrier cells and end regions. The device is 27 m long and the volume of the vacuum vessel is 150 m³. The main plasma production, ICRF heating of the plasma, and hydrogen gas puffing are applied in the central cell. The anchor cells have a minimum-B configuration and maintain the stability of the plasma. The present experiment employed two types of ICRF heating systems: one that produced the plasma and heated it in the anchor cells, and another that heated the

author's e-mail: nojiri_kunpei@prc.tsukuba.ac.jp

^{*}) This article is based on the presentation at the 12th International Conference on Open Magnetic Systems for Plasma Confinement (OS2018).

plasma in the central cell. Hereafter, the former and latter are referred to as RF1 and RF2, respectively. The standard discharge in GAMMA 10/PDX employs both RF1 and RF2.

In the west-end region, an LP and an ion energy analyzer named end loss ion energy analyzer [10, 12] are installed. The analyzer is hereinafter referred to IEA. The LP is installed near the roof target of the divertor simulation experimental module (D-module [10, 11]; see Fig. 1 (c)). The vertical position of the D-module and the probe are adjustable. The tungsten LP electrode is 1.5 mm in diameter and 1.1 mm long. The IEA is schematized in Fig. 1 (d). Ions with lower energy than the effective potential energy at the ion repeller grid are reflected and collected at the collector plate. In this study, $T_{i||}$ was evaluated by Maxwellian fitting of the energy spectra measured by the IEA. When two components of the Maxwellian distribution were identifiable, we calculated the effective $T_{i||}$ from the relative densities of the components.

2.2 Evaluation of $\gamma T_{i||}$ using a Langmuir probe

The ion and electron saturation currents (I_{is} and I_{es} , respectively) of the hydrogen plasma are respectively given by

$$I_{is} = \frac{1}{2} S n_e \sqrt{\frac{kT_e + \gamma kT_{i||}}{m_i}}, \quad (1)$$

$$I_{es} = \frac{1}{4} S n_e \sqrt{\frac{8kT_e}{\pi m_e}}, \quad (2)$$

where S is the effective probe surface area, and m_i and m_e are the ion and electron masses, respectively. The surface areas of I_{is} and I_{es} are assumed identical. The coefficient 1/2 of Eq. (1) is the ratio of the density at the sheath edge

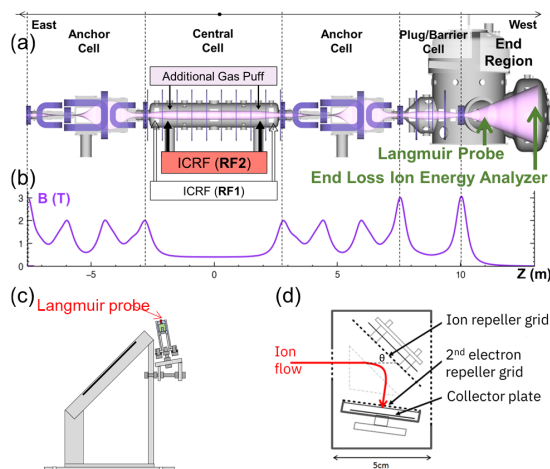


Fig. 1 Schematics of (a) part of the GAMMA 10/PDX tandem mirror, (b) magnetic field distribution in part (a), (c) Langmuir probe installed near the roof target, and (d) end-loss ion energy analyzer.

to the upstream density derived from the conservative form of the momentum equation [13]. The values of I_{is} , I_{es} and n_e can be obtained from the LP current-voltage characteristics. In this study, n_e was evaluated from I_{es} and T_e using Eq. (2). Combining Eqs. (1) and (2), $\gamma T_{i||}$ is calculated as follows:

$$\gamma T_{i||} = \left[\frac{2m_i}{\pi m_e} \left(\frac{I_{is}}{I_{es}} \right)^2 - 1 \right] T_e. \quad (3)$$

3. Experimental Results and Discussion

3.1 T_i variation by ICRF heating and additional gas puff in the central cell

In the experiment, the $T_{i||}$ of the end-loss plasma was varied by applying RF2 and an additional hydrogen gas puff in the central cell. The plasma discharge was conducted with or without RF2 (RF1 was applied in both discharges). The additional gas in the central cell was supplied from time $t = 160$ to $t = 240$ ms at a plenum pressure of 70 Torr. Figure 2 shows typical time evolutions of the diamagnetism (DM_{CC}) in the central cell (a), electron line density (NL_{CC}) in the central cell (b), and the $T_{i||}$ (c) and particle flux (d) measured by the IEA ($T_{i||,IEA}$ and $\Gamma_{i||,IEA}$, which mean $T_{i||}$ and $\Gamma_{i||}$ at the end plate, respectively). The temporal evolutions of DM_{CC} and NL_{CC} were those of a typical discharge. The $T_{i||,IEA}$ and $\Gamma_{i||,IEA}$ data were aver-

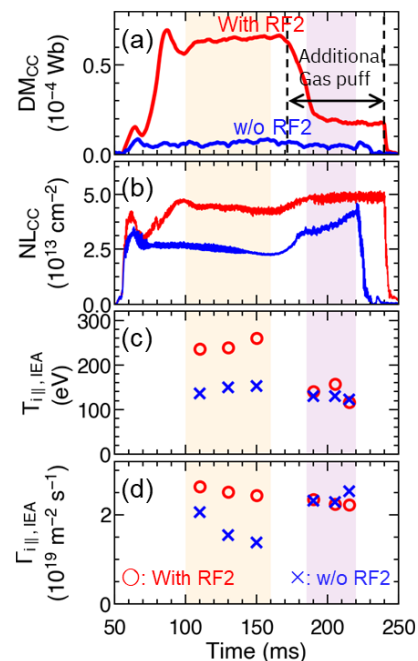


Fig. 2 Time evolution of (a) diamagnetism and (b) electron line density of plasma in the central cell; (c) ion temperature parallel to the magnetic field $T_{i||}$ and (d) ion particle flux $\Gamma_{i||}$ at the end plate, measured by the IEA in the west end region. Red lines and circles: with RF2; blue lines and crosses: without RF2.

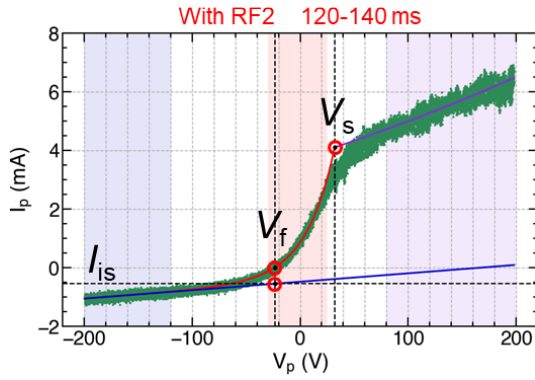


Fig. 3 Typical current-voltage characteristics of the LP.

aged over three similar discharges. The DM_{CC} was higher with the RF2 than without the RF2, indicating a higher T_i of the central plasma in the former operation. Supplying additional gas reduced the DM_{CC} in the setup with RF2. The NL_{CC} was also higher with the RF2 than without the RF2. In both discharges, the additional hydrogen gas increased the NL_{CC} . In the west-end region without the additional gas, $T_{i||,IEA}$ and $\Gamma_{i||,IEA}$ with the RF2 were higher than those without RF2. The $T_{i||,IEA}$ with RF2 was higher than without RF2 by virtue of a high-temperature component that was not identified in the absence of RF2. The details are described in Sec. 3.3. The gas supply in the central cell reduced the $T_{i||,IEA}$ and $\Gamma_{i||,IEA}$ in the RF2 operation. In the no-RF2 operation, the additional gas slightly decreased the $T_{i||,IEA}$ and increased the $\Gamma_{i||,IEA}$. Both values became similar to those with the RF2. In the absence of the gas puff, the $T_{i||,IEA}$ values with and without the RF2 were ~ 240 eV and ~ 140 eV, respectively. When the gas was supplied, $T_{i||,IEA}$ was ~ 130 eV in both the RF2 and no-RF2 operations.

3.2 Langmuir probe analysis

Figure 3 shows the typical LP current (I_p)-voltage (V_p) characteristics measured at $t = 120$ - 140 ms during the shots of IEA in the RF2 operation. The I_p - V_p characteristics were analyzed by the standard procedure described in Ref. [14]. To avoid the error resulting from sheath expansion, I_{is} was derived from the linearly fitted current at $V_p = V_f$, where V_f is the floating potential. Meanwhile, the electron current I_{es} was determined at $V_p = V_s$, where V_s is the space potential. Having determined I_{es} and T_e , n_e was determined by rearranging Eq. (2). To compensate the magnetic field effect on the collection area of the electrons (and consequently on n_e), S was taken as the projected area of the magnetic field line on the probe surface.

Figures 4 (a)-(e) show the time evolutions of T_e , n_e , I_{is} and I_{es} , and $(I_{is}/I_{es})^2$ obtained from the LP. Each dataset was measured during the shots of the IEA, and the error bars were obtained from the fitting errors. In the period without the additional gas puff in the central cell, T_e was ~ 30 eV with the RF2 and ~ 20 eV without the RF2. During

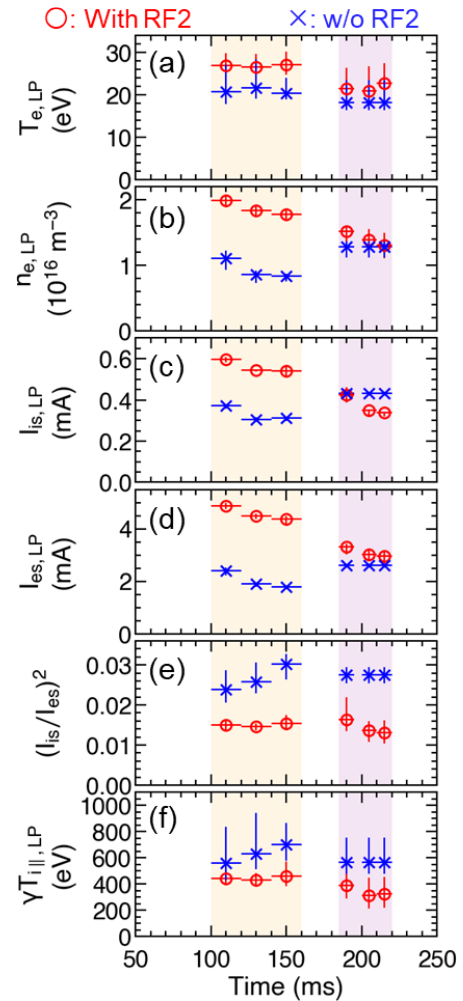


Fig. 4 Time evolutions of (a) T_e , (b) n_e , (c) I_{is} , (d) I_{es} , (e) $(I_{is}/I_{es})^2$, (f) $\gamma T_{i||}$ evaluated using a Langmuir probe. Red circles: with RF2; blue crosses: without RF2.

the same period, n_e was $\sim 2 \times 10^{16} \text{ m}^{-3}$ and $\sim 1 \times 10^{16} \text{ m}^{-3}$ with and without the RF2, respectively. In both discharges, T_e decreased when the additional gas was supplied. At that time, n_e slightly decreased with the RF2 and slightly increased without the RF2, such that the two n_e converged. In the period without the gas puff, I_{is} and I_{es} were both higher in the RF2 than in the no-RF2 operation. When the gas was supplied, the I_{is} values in both discharges were almost identical. The determination of $\gamma T_{i||}$ in Eq. (3) crucially depends on the parameter $(I_{is}/I_{es})^2$. The square of the current ratio was lower with the RF2 than without the RF2 throughout the discharge. Substituting the above parameters in Eq. (3), we obtain $\gamma T_{i||}$. Figure 4 (f) shows the time evolution of $\gamma T_{i||}$ obtained from the LP ($\gamma T_{i||,LP}$). When the gas was supplied in the central cell, $\gamma T_{i||,LP}$ decreased over time with the RF2, but was relatively stable without the RF2. Similar tendencies were observed in $T_{i||}$ evaluated by the IEA. On the other hand, in the period without the additional gas puff ($t = 100$ - 160 ms), $\gamma T_{i||,LP}$ with the RF2 was lower than without the RF2. The val-

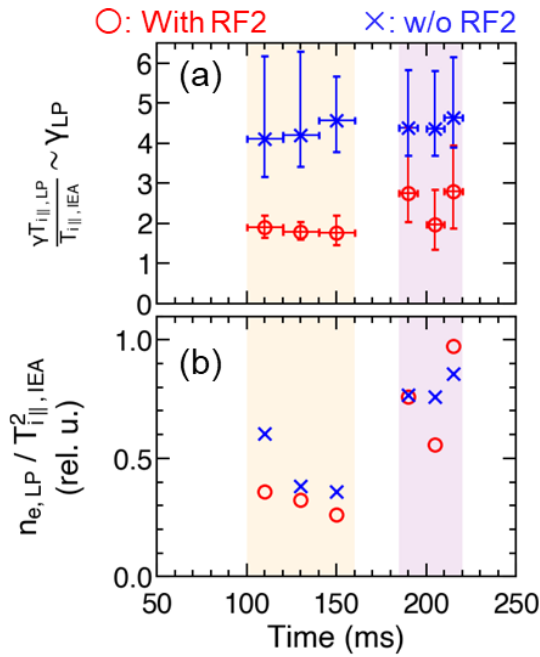


Fig. 5 Time evolutions of (a) evaluated ion polytropic coefficient and (b) $n_{e,LP}/T_{||,IEA}^2$, which is proportional to collisionality. Red circles: with RF2; blue crosses: without RF2.

ues of $\gamma T_{||,LP}$ with and without RF2 were ~ 440 eV and ~ 620 eV, respectively.

3.3 Evaluation of γ using the Langmuir probe and ion energy analyzer

To obtain γ , we assumed that the $T_{||}$ values near the LP and IEA were nearly identical, and divided $\gamma T_{||,LP}$ by $T_{||,IEA}$. Figure 5 (a) shows the time evolution of the evaluated γ . In the RF2 operation, γ was ~ 1.8 in the first period, increasing to ~ 2.5 during the gas supply. In no-RF2 operation, γ was approximately 4.4. Since there are large errors in γ due to the fitting errors of the LP, we qualitatively analyze γ with and without RF2 in the period without the additional gas.

First, we consider the characteristics of γ in the widely used plasma fluid model [2,3,13]. In this model, γ depends on the ion-ion collisionality $L/\lambda_{i-1} \propto n/T_i^2$. As n/T_i^2 increases, γ decreases from 3 to 1. Figure 5 (b) shows the time evolution of $n_{e,LP}/T_{||,IEA}^2$, the quotient of n_e measured by the LP and $T_{||,IEA}^2$ measured by the IEA. The $n_{e,LP}/T_{||,IEA}^2$ values were almost unchanged by the additional RF2 system. The collision times in both cases (with and without the RF2) were ~ 400 ms or longer. As the collision time markedly exceeded the discharge time (200 ms), the plasmas in both cases were always collisionless. Therefore, the different γ values between the RF2 and no-RF2 operations were caused by other factors.

Next, we consider the effect of the high-temperature component of the ions on γ , mentioned in Ref. [9]. The

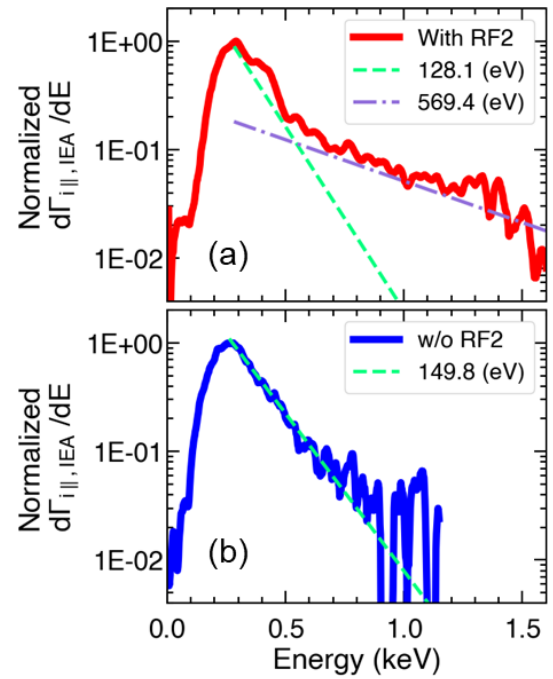


Fig. 6 Normalized ion energy spectra (a) with RF2 and (b) without RF2, measured by the IEA. The normalization factor was the peak value of the corresponding spectrum.

authors of [9] suggested that a high T_i component in collisionless plasma would reduce γ below its value in the widely used model. Figures 6 (a) and (b) show the energy spectra obtained by the IEA in the RF2 and no-RF2 operations, respectively. The spectra were collected from $t = 120$ to 140 ms and normalized by their peak values. Without RF2, the spectrum was a single Maxwellian distribution of $T_{||} \sim 150$ eV, whereas the RF2 spectrum was the convolution of two Maxwellian distributions of $T_{||} \sim 130$ eV and ~ 570 eV. Together with the result in Ref. [9], this result suggests that γ was lowered by a high-temperature ion component resulting from the ICRF heating.

Without the RF2, the evaluated γ exceeded 3.0, the upper limit in the plasma fluid model. In order to clarify the reason for this discrepancy, it requires a more quantitative investigation. In this study, we assumed that the $T_{||}$ values were almost the same at the LP and the IEA. If there was a large $T_{||}$ gradient in the setup without RF2, the evaluated γ would change. The spatial distribution of $T_{||}$ can be investigated using numerical simulations. In addition, the measurements were performed in an expanding magnetic field. In such a magnetic field, ion flow acceleration [15] and a diamagnetic property of electrons [16] have been confirmed in the lower T_i plasma. Elucidating these effects in the high $T_{||}$ plasma also requires a kinetic simulation. These investigations are future works.

4. Summary

We experimentally investigated the effect of high T_i on the ion polytropic coefficient (γ). Utilizing the high T_i plasma and ICRF heating system in the GAMMA 10 tandem mirror, the $T_{i||}$ was varied in the end region of GAMMA 10, and its effect on γ was evaluated. The $\gamma T_{i||}$ was determined using a LP, assuming that the ion drift speed was the sound speed. The $T_{i||}$ was evaluated by an IEA installed downstream of the LP. Assuming almost identical $T_{i||}$ values at the LP and IEA positions, γ was evaluated by dividing $\gamma T_{i||,LP}$ by $T_{i||,IEA}$. The $T_{i||}$ in the end region was varied by applying ICRF heating (RF2), and supplying an additional gas puff in the central cell. The $T_{i||,IEA}$ was higher with the RF2 than without the RF2, and its time evolution was similar to that of the obtained $\gamma T_{i||,LP}$. The evaluated γ was lower with the RF2 than without the RF2. In a widely used plasma fluid model, γ depends on the ion-ion collisionality; however, the plasmas in the present study were collisionless in both the RF2 and no-RF2 operations. In the RF2 operation, the ion energy spectra obtained by the IEA had a high $T_{i||}$ component. The value of γ evaluated in this experiment might have been lowered under the effect of a high-temperature ion component resulting from ICRF heating, as also mentioned in [9].

Acknowledgments

This study was performed with the support of NIFS Collaborative Research Program (NIFS16KUGM119).

- [1] D. Bohm, *The Characteristics of Electrical Discharges in Magnetic Fields*, edited by A. Guthry and R.K. Wakerling (McGraw-Hill, New York, 1949).
- [2] E. Zawaideh *et al.*, *Phys. Fluids* **29**, 463 (1986).
- [3] K.-U. Riemann, *J. Phys. D: Appl. Phys.* **24**, 493 (1991).
- [4] S. Robertson, *Phys. Plasmas* **16**, 103503 (2009).
- [5] H. Ghomi and M. Khoramabadi, *J. Plasma Phys.* **76**, 247 (2010).
- [6] J. Ou and J. Yang, *Phys. Plasmas* **19**, 113504 (2012).
- [7] M.M. Hatami, *Phys. Plasmas* **20**, 083501 (2013).
- [8] J.I.F. Palop *et al.*, *J. Phys. D: Appl. Phys.* **37**, 863 (2004).
- [9] B. Lin *et al.*, *Phys. Plasmas* **23**, 083508 (2016).
- [10] Y. Nakashima *et al.*, *Nucl. Fusion* **57**, 116033 (2017).
- [11] Y. Nakashima *et al.*, *Fusion. Sci. Technol.* **68**, 28 (2015).
- [12] Y. Sakamoto *et al.*, *Rev. Sci. Instrum.* **66**, 4928 (1995).
- [13] P.C. Stangeby, *The Plasma Boundary of Magnetic Fusion Devices* (IOP, Bristol, 2000).
- [14] I.H. Hutchinson, *Principles of Plasma Diagnostics second edition* (Cambridge University Press, 2002).
- [15] M. Inutake *et al.*, *J. Plasma Fusion Res.* **78**, 1352 (2002).
- [16] K. Takahashi *et al.*, *Phys. Rev. Lett.* **120**, 045001 (2018).